

Masato Saitoh : Lumped parameter models representing impedance functions at the interface of a rod on a viscoelastic medium, *Journal of Sound and Vibration* (in press, available on line), 2010. 11.

Lumped Parameter Models Representing Impedance Functions at the Interface of a Rod on a Viscoelastic Medium

Masato Saitoh

*Graduate School of Science and Engineering, Saitama University
255 Shimo-Okubo, Sakura-Ku, Saitama, Japan*

Tel.: +81-48-858-3560

E-mail address: saity@mail.saitama-u.ac.jp

Abstract

In this study, a lumped parameter model that properly simulates the impedance characteristics at the extremity of a uniform, isotropic, homogeneous rod on a viscoelastic medium is proposed. The lumped parameter model consists of springs, dashpots, and so called “gyromass elements”. The gyromass elements generate a reaction force proportional to the relative acceleration of the nodes between which they are placed. This model consists of units arranged in series, each unit consisting of a spring, a damper, and a gyromass element arranged in parallel. A formula is proposed for determining the properties of the elements in the units calculated from a closed-form solution based on a modal expansion. The impedance function simulated by the proposed model shows good agreement with the rigorous impedance function derived from the differential equation of motion of the rod. The results obtained by employing this model in some example applications show that the accuracy of the model is appreciably high when compared with conventional finite element models. A great advantage of this model is that a significant reduction of the number of degrees of freedom can be achieved for solving recent vibration problems with high-frequency excitations, such as ultrasonic vibrations.

Keywords/ homogeneous rod, impedance functions, lumped parameter models, dynamic response, viscoelastic media

Masato Saitoh : Lumped parameter models representing impedance functions at the interface of a rod on a viscoelastic medium, *Journal of Sound and Vibration* (in press, available on line), 2010. 11.

1. Introduction

Structures such as industrial machines, water ducts, massive slabs, bridges etc. are often connected or supported by uniform rods resting on viscoelastic media. In principle, various vibrations occur in rods, such as tension, shear, and torsion, interacting with the viscoelastic medium due to the vibration of the structure attached to them. In this case, each rod behaves as a dynamic stiffness and a damping at the end where it connects with the vibrating structure (in this study, called “interface”). Generally, the dynamic stiffness and damping characteristics are represented by a so called “impedance function”.

A number of studies associated with impedance functions have been conducted for several decades. In a pioneer study, Novak [1] investigated an elastic rod embedded in a homogeneous medium modeled as a Winkler medium resisting the rod motion using continuously-distributed, frequency-independent springs and dashpots. For more a realistic representation of the subgrade reaction of the medium in the model, frequency-dependent springs and dashpots proposed by Baranov [2] were incorporated into several studies (Novak [3], Novak and Howell [4], Novak et al. [5], Gazetas and Makris [6]). These studies showed that the impedance functions of rods connecting with springs and dashpots have frequency-dependent characteristics; namely, the stiffness and damping change due to a change in the excitation frequency at the interface.

In actuality, however, frequency-dependent impedance characteristics have been a serious hindrance in numerical computations for obtaining the dynamic response of structures connected with rods when material nonlinearities such as cracking, yielding, and collapse of vibrating structures occur.

Lumped parameter models (LPMs) are powerful tools for solving this problem (Barros and Luco [7], Wolf [8, 9], Wu and Lee [10], and Andersen [11]). In general, LPMs consist of springs, dashpots, and masses. A particular combination of elements allows simulation of a frequency-dependent impedance characteristic, even though each element has a frequency-independent coefficient. It is apparent, therefore, that the LPMs can easily be incorporated into a conventional numerical analysis in the time domain, even under nonlinear conditions. Furthermore, in recent work by Saitoh [12], a newly developed element called a “gyro-mass” was incorporated into an LPM for a more accurate representation of frequency-dependent impedance functions with a small number of elements, instead of using a general mass. The gyromass element generates a reaction force proportional to the relative acceleration of the nodes between which it is placed. The study showed that an LPM with the gyro-mass (GLPM) accurately simulated impedance functions showing complicated oscillations with frequency.

There have been a number of studies dealing with longitudinally vibrating elastic rods with

Masato Saitoh : Lumped parameter models representing impedance functions at the interface of a rod on a viscoelastic medium, *Journal of Sound and Vibration* (in press, available on line), 2010. 11.

various boundary conditions (e.g., Hizal and Gürgöze [13], Gürgöze and Inceoğlu [14], Li et al. [15], Candan and Elishakoff [16], Yüksel and Gürgöze [17], and Erol and Gürgöze [18]). Hizal and Gürgöze [13] proposed an LPM of a longitudinally vibrating elastic rod with a viscous damping element placed at the intermediate span. Their LPM can be used to represent the impedance characteristic at the extremity of the rod when connected with a vibrating structure. However, to the best of the author's knowledge, only a limited number of studies on LPMs associated with rods have been presented despite their usefulness in various technological applications.

Here, a GLPM representing the impedance function at the interface of the mechanical system shown in Fig. 1, which is a longitudinally vibrating elastic rod resting on continuously-distributed springs and dashpots (the Kelvin–Voigt model is assumed as a viscoelastic medium), is presented. One end of the rod is assumed to be connected with a spring, in accordance with actual rods frequently employed in a wide range of applications. It is apparent that, in principle, the GLPM derived here is also applicable to other vibrating modes of rods deformed in transverse shear and torsion, respectively. The objectives of this study are: 1) To formulate a GLPM with gyro-mass elements by means of a closed-form solution of the impedance function based on a modal expansion; 2) to verify the accuracy of the proposed GLPM compared with a rigorous solution and conventional finite element models (FEMs) in the frequency domain through two example applications; and 3) to show an advantage of the proposed GLPM for recent vibration problems where an extremely high-frequency region, such as ultrasonic excitations, is dealt with: a significant reduction of the number of degrees of freedom (DOFs) for representing the impedance function of rods can be achieved.

2. Formulation of Rigorous Solution and GLPM Based on Modal Expansion

2.1. Formulation of Rigorous Solution

The mechanical system to be studied is shown in Fig. 1. A uniform, isotropic, homogeneous, elastic, horizontal rod of cross-sectional area A is supported by continuously-distributed springs and dashpots. One end of the rod is longitudinally restrained by a spring k_b . A one-dimensional coordinate system z is assumed. An external force $P_0 \exp(i\omega t)$ is applied to the rod at the free end, where ω is the circular frequency of the external force. The length of the rod is l . The governing equation of motion is

Masato Saitoh : Lumped parameter models representing impedance functions at the interface of a rod on a viscoelastic medium, *Journal of Sound and Vibration* (in press, available on line), 2010. 11.

$$EAu''(z,t) - \rho A \ddot{u}(z,t) - k^* u(z,t) = 0, \quad (1)$$

where the dots and primes denote partial derivatives with respect to time t and position coordinate z , respectively. E and ρ are the elastic modulus and mass density, respectively, and u is the displacement of the rod. k^* is a unit of a spring k and a dashpot c per unit length arranged in parallel, according to the Kelvin–Voigt model (i.e., $k^* = k + i\omega c$). The boundary conditions of the rod are expressed in the following form:

$$\text{at } z = 0: \quad EAu' = -P_0 e^{i\omega t}, \quad (2)$$

$$\text{at } z = l: \quad EAu' + k_b u = 0. \quad (3)$$

The general solution of Eq. 1 is

$$u(z,t) = (A_1 e^{\lambda z} + A_2 e^{-\lambda z}) e^{i\omega t}. \quad (4)$$

Substituting Eq. 4 into Eqs. 2 and 3 gives the constants A_1 and A_2 in terms of λ as follows:

$$A_1 = \frac{e^{-\lambda l} (-\lambda + k_b/EA)}{2\lambda (\lambda EA \sinh \lambda l + k_b \cosh \lambda l)} P_0, \quad (5)$$

$$A_2 = \frac{e^{\lambda l} (\lambda + k_b/EA)}{2\lambda (\lambda EA \sinh \lambda l + k_b \cosh \lambda l)} P_0, \quad (6)$$

where

$$\lambda = \sqrt{\frac{k^* - \rho A \omega^2}{EA}}. \quad (7)$$

Substituting $z = 0$ into Eq. 4 gives the response displacement at the interface of the rod as follows:

$$u(0,t) = \bar{u} e^{i\omega t}, \quad (8)$$

Masato Saitoh : Lumped parameter models representing impedance functions at the interface of a rod on a viscoelastic medium, *Journal of Sound and Vibration* (in press, available on line), 2010. 11.

where

$$\bar{u} = \frac{P_0 l}{EA} \frac{\lambda \cosh \lambda l + \frac{k_b}{EA} \sinh \lambda l}{\lambda l \left(\lambda \sinh \lambda l + \frac{k_b}{EA} \cosh \lambda l \right)}. \quad (9)$$

Consequently, dividing the external force $P_0 e^{i\omega t}$ by the amplitude of the response displacement $\bar{u} e^{i\omega t}$ yields the impedance function at the interface, K^* , as follows:

$$K^* = k_0 \bar{K}^*, \quad (10)$$

where k_0 is the static stiffness at the interface of an isolated rod without springs and dashpots distributed along the rod, given by

$$k_0 = \frac{EA}{l}. \quad (11)$$

Here, the impedance function normalized by the static stiffness k_0 (hereinafter, called the “normalized impedance function”) is expressed as follows:

$$\bar{K}^* = \bar{K}^*(a_0) = \frac{\eta (\eta \sinh \eta + s_b \cosh \eta)}{\eta \cosh \eta + s_b \sinh \eta}, \quad (12)$$

where

$$s_b = \frac{k_b}{k_0},$$

$$\eta = \sqrt{s_k + ia_0 s_c - a_0^2},$$

$$s_k = \frac{kl}{k_0},$$

$$s_c = \frac{cl}{k_0} \left(\frac{c_p}{l} \right).$$

Masato Saitoh : Lumped parameter models representing impedance functions at the interface of a rod on a viscoelastic medium, *Journal of Sound and Vibration* (in press, available on line), 2010. 11.

Here, $c_p (= \sqrt{E/\rho})$ is the velocity of the wave propagation along the rod, and $a_0 (= \omega l/c_p)$ is the normalized frequency.

It is apparent that the rigorous impedance function at the interface of the rod is frequency-dependent because Eq. 12 is a function of the excitation frequency ω .

2.2. Formulation of Solution Based on Modal Expansion

Modal expansion techniques are other methodologies to solve this problem. Here, the following governing equation of motion is to be solved:

$$EAu''(z,t) - \rho A\ddot{u}(z,t) - k^*u(z,t) = -P_0\delta(z)e^{i\omega t}. \quad (13)$$

In the present study, an approximate modal expansion method is used to obtain the relation between the harmonic external force and the response displacement at the interface. In this method, the mode shapes of a solitary rod without the restriction of the springs and dashpots along the rod are used to express the response displacement of the rod satisfying Eq. 13. This method was pioneered by Tajimi [19] and Nogami and Novak [20] and has been quite successfully used for solving the response displacement of rods embedded in an elastic continuum.

The partial differential equation for determining the mode shapes of the solitary rod is as follows:

$$EAu''(z,t) - \rho A\ddot{u}(z,t) = 0. \quad (14)$$

The following response displacement of the rod is assumed:

$$u(z,t) = e^{\beta z} e^{i\omega t}. \quad (15)$$

Substituting Eq. 15 into Eq. 14 leads to the following general solution:

$$u(z,t) = \left(C \sin \frac{\omega}{c_p} z + D \cos \frac{\omega}{c_p} z \right) \cdot e^{i\omega t}. \quad (16)$$

Masato Saitoh : Lumped parameter models representing impedance functions at the interface of a rod on a viscoelastic medium, *Journal of Sound and Vibration* (in press, available on line), 2010. 11.

Eq. 16 satisfies the following boundary conditions:

$$\text{at } z = 0: \quad EAu' = 0, \quad (17)$$

$$\text{at } z = l: \quad EAu' + k_b u = 0. \quad (18)$$

Substituting Eq. 16 into Eqs. 17 and 18 leads to

$$u(z, t) = \sum_{i=1}^{\infty} D_i \cos \frac{\omega_i}{c_p} z \cdot e^{i\omega t}, \quad (19)$$

where ω_i satisfies

$$\tan a_i = \frac{s_b}{a_i}, \quad (20)$$

where

$$a_i = \frac{\omega_i l}{c_p}.$$

The modal coefficients D_i are determined by substituting Eq. 19 into Eq. 13. Consequently, the following general solution of the displacement of the rod satisfying Eq. 13 can be obtained:

$$u(z, t) = \sum_{i=1}^{\infty} \frac{2}{k_0} \frac{1}{s_k + a_i^2 + ia_0 s_c - a_0^2} \frac{\frac{1}{2a_i} \sin 2a_i + 1}{\cos a_i \left(\frac{z}{l} \right)} \cdot P_0 e^{i\omega t}. \quad (21)$$

Accordingly, the normalized impedance function at the interface of the rod ($z=0$) can be obtained from Eq. 21:

Masato Saitoh : Lumped parameter models representing impedance functions at the interface of a rod on a viscoelastic medium, *Journal of Sound and Vibration* (in press, available on line), 2010. 11.

$$\bar{K}^*(a_0) = \frac{K^*}{k_0} = \frac{2}{1 + \sum_{i=1}^{\infty} \frac{\frac{1}{2a_i} \sin 2a_i + 1}{s_k + a_i^2 + ia_0 s_c - a_0^2}}. \quad (22)$$

2.3. Formulation of LPM with Gyro-Mass (GLPM)

Based on Eq. 22, the impedance function of the rod can also be expressed as follows:

$$\begin{aligned} K^*(a_0) &= \frac{1}{\sum_{i=1}^{\infty} \frac{1}{K_i + ia_0 \tilde{C}_i - a_0^2 \tilde{M}_i}} \\ &= \frac{1}{\sum_{i=1}^{\infty} \frac{1}{K_i + i\omega C_i - \omega^2 \bar{M}_i}} \\ &= \frac{1}{\frac{1}{K_1 + i\omega C_1 - \omega^2 \bar{M}_1} + \frac{1}{K_2 + i\omega C_2 - \omega^2 \bar{M}_2} + \dots} \end{aligned} \quad (23)$$

where

$$K_i = \frac{k_0}{2} (s_k + a_i^2) \left(\frac{1}{2a_i} \sin 2a_i + 1 \right),$$

$$\tilde{C}_i = \frac{k_0}{2} s_c \left(\frac{1}{2a_i} \sin 2a_i + 1 \right),$$

$$\tilde{M}_i = \frac{k_0}{2} \left(\frac{1}{2a_i} \sin 2a_i + 1 \right).$$

$$C_i = \left(\frac{l}{c_p} \right) \tilde{C}_i$$

$$\bar{M}_i = \left(\frac{l}{c_p} \right)^2 \tilde{M}_i$$

Masato Saitoh : Lumped parameter models representing impedance functions at the interface of a rod on a viscoelastic medium, *Journal of Sound and Vibration* (in press, available on line), 2010. 11.

From Eq. 23, it is found that the impedance function can be formulated by a set of units arranged in series, each unit consisting of a spring K_i , a dashpot C_i , and a so-called gyro-mass element \bar{M}_i arranged in parallel, as shown in Fig. 2. The case shown in the figure, where the maximum number of units is N , is described by an approximation of the infinite series in Eq. 23. It is apparent that the number N is identical to the maximum number of modes to be considered in the LPM. Although the element \bar{M}_i has the same dimension as ordinary mass, the element should generate a reaction force proportional to the relative acceleration of the two nodes between which it is placed. This gyro-mass element was first proposed and initially used for expressing frequency-dependent impedance functions by Saitoh [12]. Fig. 3 (a) shows one of the mechanical analogies described in his paper for realizing the gyro-mass. He explained this analogy as follows. The mechanical analogy consists of a rotational disk and a massless rod attached to the disk with strong friction. The disk rotates with rotational acceleration $\ddot{\theta}$ as an external force F is given to the rod. The relative acceleration of the rod \ddot{u} with respect to the fixed node at the right-hand side is geometrically related to the rotational acceleration $\ddot{\theta}$. Consequently, the following relation between the external force F and the relative acceleration \ddot{u} can be obtained:

$$F = \bar{M} \ddot{u}, \quad (24)$$

where

$$\bar{M} = \frac{J}{r^2}. \quad (25)$$

Here, r is the distance from the center of the disk to the point where the rod is attached; J is the moment of inertia of the disk; and \bar{M} is the gyro-mass generated by the rotation of the disk. Thus, the reaction force at the left-hand side of the rod is identical to the product of the gyro-mass \bar{M} and the relative acceleration \ddot{u} . This is the reason why \bar{M} is termed ‘‘gyro-mass’’, in order to distinguish it from ordinary mass. In addition, an LPM using the gyro-mass instead of a general mass is called a ‘‘GLPM’’ in the present study.

Masato Saitoh : Lumped parameter models representing impedance functions at the interface of a rod on a viscoelastic medium, *Journal of Sound and Vibration* (in press, available on line), 2010. 11.

3. Verification of GLPM in Example Applications

The effectiveness of the GLPM is verified through two example applications. First, the impedance functions of the GLPM are compared with the rigorous impedance functions obtained by Eq. 12. Second, the degree of accuracy of the GLPM is compared with that of two types of conventional FEMs: one is an FEM where the mass of the rod is constructed based on a lumped mass approach (called “FEML” in the following); the other is an FEM where the mass of the rod is constructed based on a consistent mass approach (called “FEMC” in the following).

3.1. Formulation of Conventional FEMs

A mechanical system of the FEMs is shown in Fig. 4. The rod is discretized by a set of rod elements. The stiffness matrix for each rod element can be generally described by the following formula (e.g. Thomson [21]):

$$[k_{ij}] = (n-1)k_0 \begin{bmatrix} 1 & -1 \\ -1 & 1 \end{bmatrix} \quad (26)$$

where n is the total number of DOFs; and i and j are the numbers of successive nodes in the model. The mass matrices for the elements based on a lumped mass approach and a consistent mass approach are expressed by the following formulae (e.g., Thomson [21] and Tedesco et al. [22]), respectively:

$$\text{for FEML:} \quad [m_{ij}] = \frac{\rho A l}{n-1} \begin{bmatrix} 1/2 & 0 \\ 0 & 1/2 \end{bmatrix}. \quad (27)$$

$$\text{for FEMC:} \quad [m_{ij}] = \frac{\rho A l}{n-1} \begin{bmatrix} 1/3 & 1/6 \\ 1/6 & 1/3 \end{bmatrix}. \quad (28)$$

A unit consisting of a spring k_s and a dashpot c_s representing a viscoelastic medium, is connected at the nodes of the models. They are given by

Masato Saitoh : Lumped parameter models representing impedance functions at the interface of a rod on a viscoelastic medium, *Journal of Sound and Vibration* (in press, available on line), 2010. 11.

At ends ($n \neq 1$)

Intermediate nodes ($n \neq 1, 2$)

$n = 1$

$$k_s = \frac{k_0 s_k}{2(n-1)} \quad (29)$$

$$= \frac{k_0 s_k}{n-1}$$

$$= \frac{k_0 s_k}{n}$$

At ends ($n \neq 1$)

Intermediate nodes ($n \neq 1, 2$)

$n = 1$

$$c_s = \frac{k_0 s_c}{2(n-1)} \left(\frac{l}{c_p} \right) \quad (30)$$

$$= \frac{k_0 s_c}{n-1} \left(\frac{l}{c_p} \right)$$

$$= \frac{k_0 s_c}{n} \left(\frac{l}{c_p} \right)$$

A harmonic force is applied at the free end, and then the response displacement is estimated by solving the equations of motion of the FEMs.

3.2. Verification of GLPM

In this section, two example applications are considered for verifying the accuracy of the GLPM proposed in the present study. The first example deals with the normalized properties that may be comparable to those of anchors supporting industrial machinery, such as electrical generators,

Masato Saitoh : Lumped parameter models representing impedance functions at the interface of a rod on a viscoelastic medium, *Journal of Sound and Vibration* (in press, available on line), 2010. 11.

turbines, and inverters. Anchors are sometimes embedded in holes filled with viscoelastic material for absorbing the kinetic energy originating from the machinery, as well as for properly supporting the machinery. The normalized properties used in this example are: $s_k = 0.8$; $s_c = 0.4$; and $s_b = 0.2$.

Fig. 5 shows a comparison of the real part of the impedance functions obtained from the rigorous solution and the GLPM results with different numbers of units ($N = 1, 2, 4, \text{ and } 8$). It is found that the rigorous impedance function of this example shows sharp local minima and maxima repeatedly with frequency. Fig. 5 indicates that increasing the number of units used in the GLPM tends to appreciably improve the agreement with the rigorous impedance function. The imaginary part (Fig. 6) also shows a tendency similar to the real part. The results obtained by using the FEMs with different numbers of DOFs ($n = 1, 2, 4, \text{ and } 8$) are also plotted in the figures for comparison. The results indicate that they tend to show smaller absolute values of the local minima and maxima in both the real and imaginary parts than the rigorous impedance function. The results also show that the frequencies corresponding to the local minima and maxima in the impedance functions evaluated by the FEML tend to be smaller than those evaluated by the rigorous solution, whereas the frequencies evaluated by the FEMC tend to shift to values larger than those evaluated by the rigorous solution. It is found that the impedance functions of the GLPM show better agreement with the rigorous solutions of these conventional FEMs. It is noteworthy that, despite the better accuracy of the GLPM, the number of elements used in the GLPM is always smaller than that of the conventional FEMs in these comparisons.

The second example deals with the normalized properties associated with those of shear keys embedded in bases for resisting shear forces transmitted from machines, such as transmissions and gear boxes, for instance. Shear keys made of engineering plastic materials (e.g., POM, PMMA, and ABS etc.) are embedded in metallic bases, for example, aluminum alloy plates. In this example, shear deformation dominates in the transverse direction of a rod (shear key) as a shear force is applied to the end of the rod, as shown in Fig. 7. Therefore, springs and dashpots along the rod resist the deformation in the transverse direction, whereas the spring at the end of the rod also resists the movement in the same direction. The normalized properties used in this example are: $s_k = 7$; $s_c = 2.1$; and $s_b = 0.7$.

Figs. 8 and 9 show that the impedance functions obtained from the rigorous solution in this example moderately oscillate with frequency owing to the larger effects of the springs and dashpots along the rod than those in the first example. The accuracy of the impedance functions of the GLPM tend to be improved gradually from the lower frequency region to the higher frequency region by increasing the number of units from $N = 1$ to 16. The reason for this is that each unit of the GLPM is directly associated with a particular mode: the modes arrayed from

Masato Saitoh : Lumped parameter models representing impedance functions at the interface of a rod on a viscoelastic medium, *Journal of Sound and Vibration* (in press, available on line), 2010. 11.

lower frequency to higher frequency as expressed in Eq. 23. Accordingly, the accuracy of the impedance functions is improved from the lower frequency with an increasing number of units. This tendency can also be seen in the first example.

In contrast, the accuracy of the FEMs tends to be improved gradually over a wide frequency range by increasing the number of DOFs from $n=1$ to 16. The results show that marked differences in the frequencies corresponding to the local maxima and minima still remain in the case of $n=16$, as well as differences in the amplitude of oscillations in the impedance functions. From this example, it may also be concluded that the GLPM shows better agreement with the rigorous solution than the conventional FEMs.

4. Advantages of GLPMs for Recent Vibration Problems

In recent vibration problems, excitations with extremely high frequencies are often dealt with, such as ultrasonic vibrations exceeding 20 kHz induced by ultrasonic machines, such as servo-cutters, welding machines, and micro turbines. It is known that the maximum frequency of ultrasonic vibrations that recent technologies can generate is of gigahertz order. Moreover, in certain vibration problems, such as high-speed moving bullet trains interacting with rails on structures, kilohertz-order vibrations need to be considered in numerical computations. In general, rods incorporated into systems excited by high frequencies need to have a large number of DOFs for expressing their deformed shapes during excitation. Therefore, there is a strong demand for an appropriate and effective representation of rods interacting with machines and structures in high-frequency regions for efficient computation.

In general, a particular high-frequency region is rather more important than other frequency regions when solving such problems where the variance of excitation frequencies is small. It is well-known that modal analysis has been frequently applied for solving various dynamic problems where a particular frequency region is dealt with because of the fact that a small set of modes associated with the frequency region can appropriately express the dynamic characteristics of vibrating systems. In accordance with the advantage of modal analysis, a great advantage in appreciably reducing the number of DOFs of GLPMs is the fact that the units comprising the GLPMs are associated with the vibrating modes of the rod. In the following discussion, therefore, we attempt to reconstruct GLPMs where a set of selected units associated with modes in a target frequency region are used without using all modes.

Fig. 10 shows the impedance functions obtained from the GLPMs using different maximum numbers of units ($N=100$ and 200) in the first example previously shown, targeting a high-

Masato Saitoh : Lumped parameter models representing impedance functions at the interface of a rod on a viscoelastic medium, *Journal of Sound and Vibration* (in press, available on line), 2010. 11.

frequency region ranging from $a_0 = 40$ to 50. The results obtained by using the FEMC with different numbers of DOFs ($n=100$ and 200) are also plotted in the figures for comparison. Fig. 10 indicates that 200 DOFs appropriately represent the impedance functions in the target frequency region for the GLPM and the FEMC, respectively.

Fig. 11 shows a comparison of the impedance functions evaluated using three reduced GLPMs (RGLPMs): 1) a RGLPM consisting of four units associated with successive modes from 14th to 17th ranging from $a_0 = 40.85$ to 50.27; 2) a RGLPM consisting of 10 units associated with modes from 12th to 21st ranging from $a_0 = 34.56$ to 62.84; and 3) a RGLPM consisting of 16 units associated with successive modes from 10th to 25th ranging from $a_0 = 28.28$ to 75.40.

The results indicate that, as a whole, the impedance functions of all the presented RGLPMs show good agreement with those of the rigorous solution within the target frequency region ($a_0 = 40$ to 50), whereas discrepancies remain around the local minima and maxima in the impedance functions of the RGLPM with four units. Fig. 11 shows that an appreciably close agreement can be seen in the RGLPM using 10 units, whereas more accurate impedance functions can be achieved using the RGLPM with 16 units. Therefore, a set of bounded modes associated with a comprehensive frequency region is necessary to consider in RGLPMs for accomplishing satisfactorily high accuracy. That is, in this example, the minimum frequency ($a_0 = 28.28$) of the comprehensive frequency region is about 0.7 times as small as the minimum frequency ($a_0 = 40$) of the target frequency region; and the maximum frequency ($a_0 = 75.40$) is about 1.5 times as large as the maximum frequency ($a_0 = 50$) of the target frequency region.

It may be concluded, therefore, that RGLPMs appreciably reduce the DOFs of GLPMs: the DOFs of RGLPMs are markedly smaller than those of the conventional FEMs; hence, the computational domain and time can also be efficiently reduced using RGLPMs for solving recent vibration problems with high excitation frequencies.

5. Conclusions

This study proposes a lumped parameter model (LPM) that properly simulates the impedance characteristics at the extremity of a uniform, isotropic, homogeneous rod supported by continuously-distributed springs and dashpots (the Kelvin–Voigt model is assumed as a viscoelastic medium). An LPM with a so called “gyro-mass” (GLPM) is formulated by means of a closed-form solution of the impedance functions based on a modal expansion. The accuracy of

Masato Saitoh : Lumped parameter models representing impedance functions at the interface of a rod on a viscoelastic medium, *Journal of Sound and Vibration* (in press, available on line), 2010. 11.

the GLPM is verified by comparison with the rigorous solution and conventional FEMs in the frequency domain through two example applications. The results of the GLPM are in better agreement with the rigorous solution than those of the conventional FEMs despite the smaller number of elements in the GLPM compared with the FEMs. Moreover, reduced GLPMs (RGLPMs) are presented for representing impedance functions in a high-frequency region. RGLPMs appreciably reduce the number of degrees of freedom when compared with conventional FEMs so that the computational domain and time can also be efficiently reduced when solving recent vibration problems such as those involving ultrasonic vibrations.

References

- [1] M. Novak, Dynamic stiffness and damping of piles, *Canadian Geotechnical Journal*, 11, 574 – 598, 1974.
- [2] V. A. Baranov, On the calculation of excited vibrations of an embedded foundation, *Voprosy Dynamiki Prochnosti*, 14, Polytech. Inst. Riga, 195–209, 1967 (*in Russian*).
- [3] M. Novak, Vertical vibration of floating piles, *Journal of Engineering Mechanics Div., ASCE*, 103(EM1), 153–168, 1977.
- [4] M. Novak, J. F. Howell, Torsional vibration of pile foundations, *Journal of Geotechnical Engineering Div., ASCE*, 103(GT4), 271–185, 1977.
- [5] M. Novak, T. Nogami, F. Aboul-Ella, Dynamic soil reactions for plane strain case, *Journal of Engineering Mechanics Div., ASCE*, 104(EM4), 953–959, 1978.
- [6] G. Gazetas, N. Makris, Dynamic pile-soil-pile interaction part I: analysis of axial vibration, *Earthquake Engineering and Structural Dynamics*, 20, 115–132, 1991.
- [7] F. C. P. de Barros, J. E. Luco, Discrete models for vertical vibrations of surface and embedded foundations, *Earthquake Engineering and Structural Dynamics*, 19, 289–303, 1990.
- [8] J. P. Wolf, *Foundation Vibration Analysis Using Simple Physical Models*, Prentice-Hall: Englewood Cliffs, NJ, 1994.
- [9] J. P. Wolf, Spring-dashpot-mass models for foundation vibrations, *Earthquake Engineering and Structural Dynamics*, 26, 931–949, 1997.
- [10] W. H. Wu, W. H. Lee, Systematic lumped-parameter models for foundations based on polynomial-fraction approximation, *Earthquake Engineering and Structural Dynamics*, 31(8), 1383–1412, 2002.
- [11] L. Andersen, Assessment of lumped-parameter models for rigid footings, *Computers and Structures*, 88(23-24), 1333-1347, 2010.

Masato Saitoh : Lumped parameter models representing impedance functions at the interface of a rod on a viscoelastic medium, *Journal of Sound and Vibration* (in press, available on line), 2010. 11.

[12] M. Saitoh, Simple Model of Frequency-Dependent Impedance Functions in Soil-Structure Interaction Using Frequency-Independent Elements, *Journal of Engineering Mechanics*, ASCE, 133(10), 1101–1114, 2007.

[13] N. A. Hizal, M. Gürgöze, Lumped parameter representation of a longitudinally vibrating elastic rod viscously damped in-span, *Journal of Sound and Vibration*, 216(2), 328–336, 1998.

[14] M. Gürgöze, S. Inceoğlu, On the vibrations of an axially vibrating elastic rod with distributed mass added in-span, *Journal of Sound and Vibration*, 230(1), 187–194, 2000.

[15] Q. S. Li, G. Q. Li, D. K. Liu, Exact solutions for longitudinal vibration of rods coupled by translational springs, *International Journal of Mechanical Science*, 42, 1135–1152, 2000.

[16] S. Candan, I. Elishakoff, Constructing the axial stiffness of longitudinally vibrating rod from fundamental mode shape, *International Journal of Solids and Structures*, 38, 3443–3452, 2001.

[17] S. Yüksel, M. Gürgöze, Continuous and discrete models for longitudinally vibrating elastic rods viscously damped in-span, *Journal of Sound and Vibration*, 257(5), 996–1006, 2002.

[18] H. Erol, M. Gürgöze, Longitudinal vibrations of a double-rod system coupled by springs and dampers, *Journal of Sound and Vibration*, 276, 419–430, 2004.

[19] H. Tajimi, Dynamic analysis of a structure embedded in an elastic stratum, *Proceedings of 4th World Conference on Earthquake Engineering*, Santiago, Chile III, 53–69, 1969.

[20] T. Nogami, M. Novak, Soil-pile interaction in vertical vibration, *Earthquake Engineering and Structural Dynamics*, 4, 277–293, 1976.

[21] W. T. Thomson, *Theory of Vibration with Applications*, fourth edition, Nelson Thornes Ltd, 2003.

[22] J. W. Tedesco, W. G. McDougal, C. A. Ross, *Structural Dynamics: theory and applications*, Addison Wesley Longman, Inc, 1999.

Masato Saitoh : Lumped parameter models representing impedance functions at the interface of a rod on a viscoelastic medium, Journal of Sound and Vibration (in press, available on line), 2010. 11.

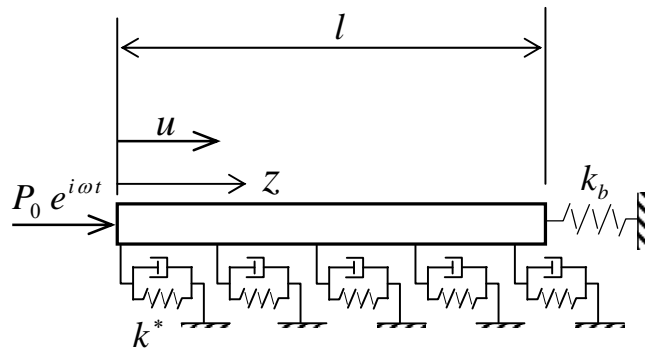


Fig. 1 Rod on viscoelastic medium considered in this study.

Masato Saitoh : Lumped parameter models representing impedance functions at the interface of a rod on a viscoelastic medium, *Journal of Sound and Vibration* (in press, available on line), 2010. 11.

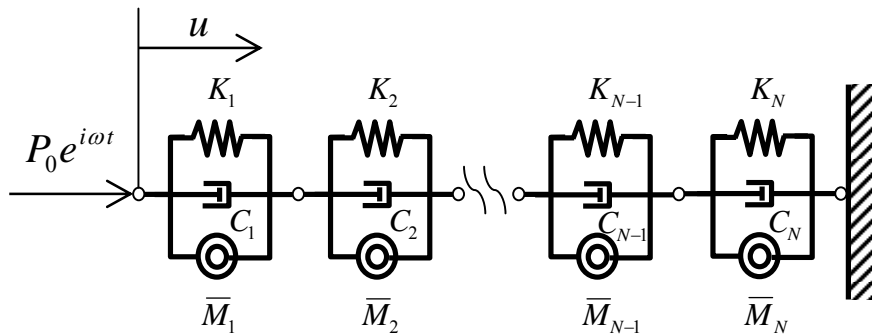


Fig. 2 Lumped parameter model (LPM) for simulating impedance function at the interface of a rod on a viscoelastic medium.

Masato Saitoh : Lumped parameter models representing impedance functions at the interface of a rod on a viscoelastic medium, *Journal of Sound and Vibration* (in press, available on line), 2010. 11.

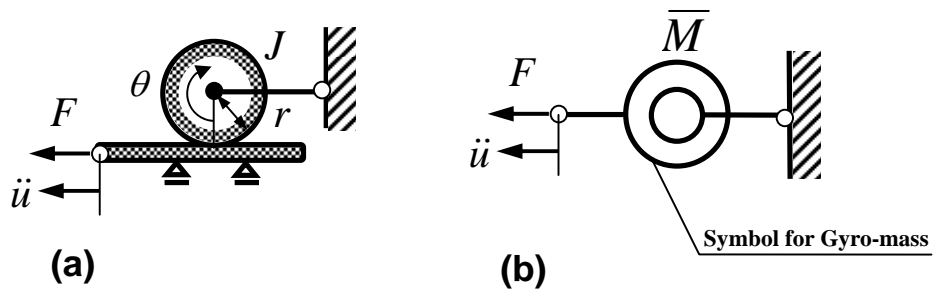


Fig. 3 Mechanical analogy of gyromass element (a) and its symbol (b), proposed by Saitoh 2007

(revised in parts).

Masato Saitoh : Lumped parameter models representing impedance functions at the interface of a rod on a viscoelastic medium, *Journal of Sound and Vibration* (in press, available on line), 2010. 11.

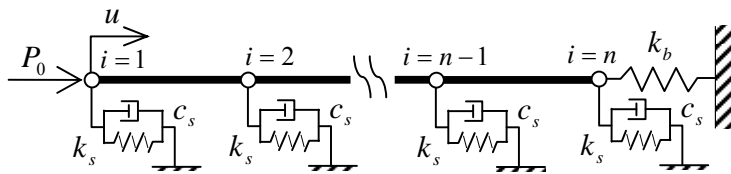
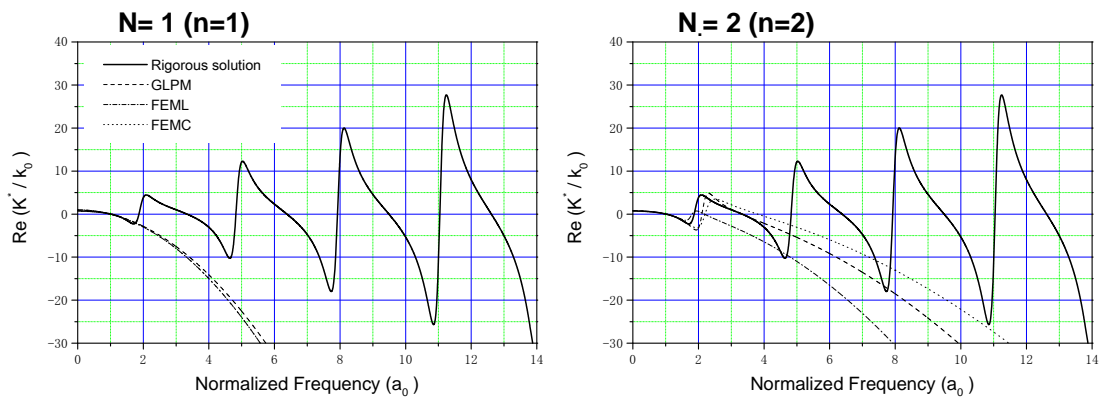


Fig. 4 Conventional finite element models (FEMs) studied (i = node number).

Masato Saitoh : Lumped parameter models representing impedance functions at the interface of a rod on a viscoelastic medium, *Journal of Sound and Vibration* (in press, available on line), 2010. 11.



N= 4 (n=4)

Masato Saitoh : Lumped parameter models representing impedance functions at the interface of a rod on a viscoelastic medium, *Journal of Sound and Vibration* (in press, available on line), 2010. 11.

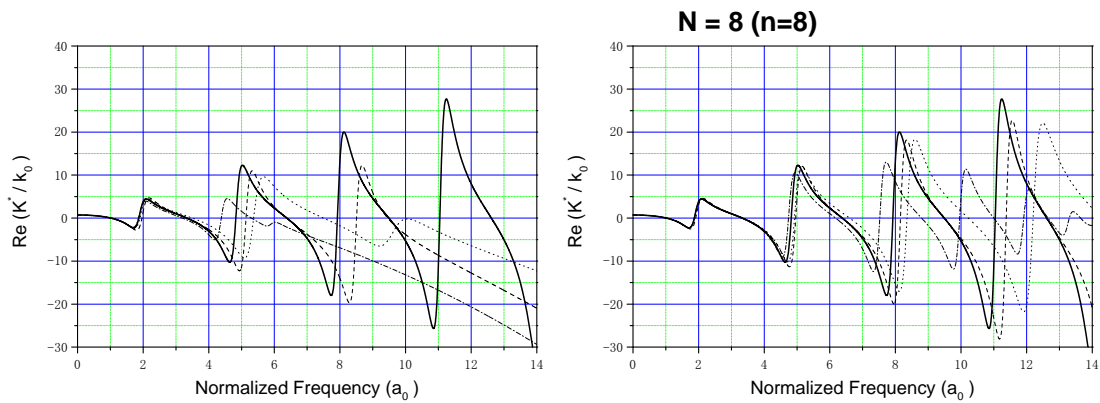


Fig. 5 Normalized impedance functions (real part) at the interface of a rod in the example application of anchors supporting vibrating machinery, using the GLPM with various maximum numbers of units (N). Also shown for comparison are results obtained with the rigorous solution and with conventional finite element models (FEML for lumped mass approach; FEMC for consistent mass approach) with various numbers of DOFs (n).

N= 1 (n=1)

N= 2 (n=2)

Masato Saitoh : Lumped parameter models representing impedance functions at the interface of a rod on a viscoelastic medium, *Journal of Sound and Vibration* (in press, available on line), 2010. 11.

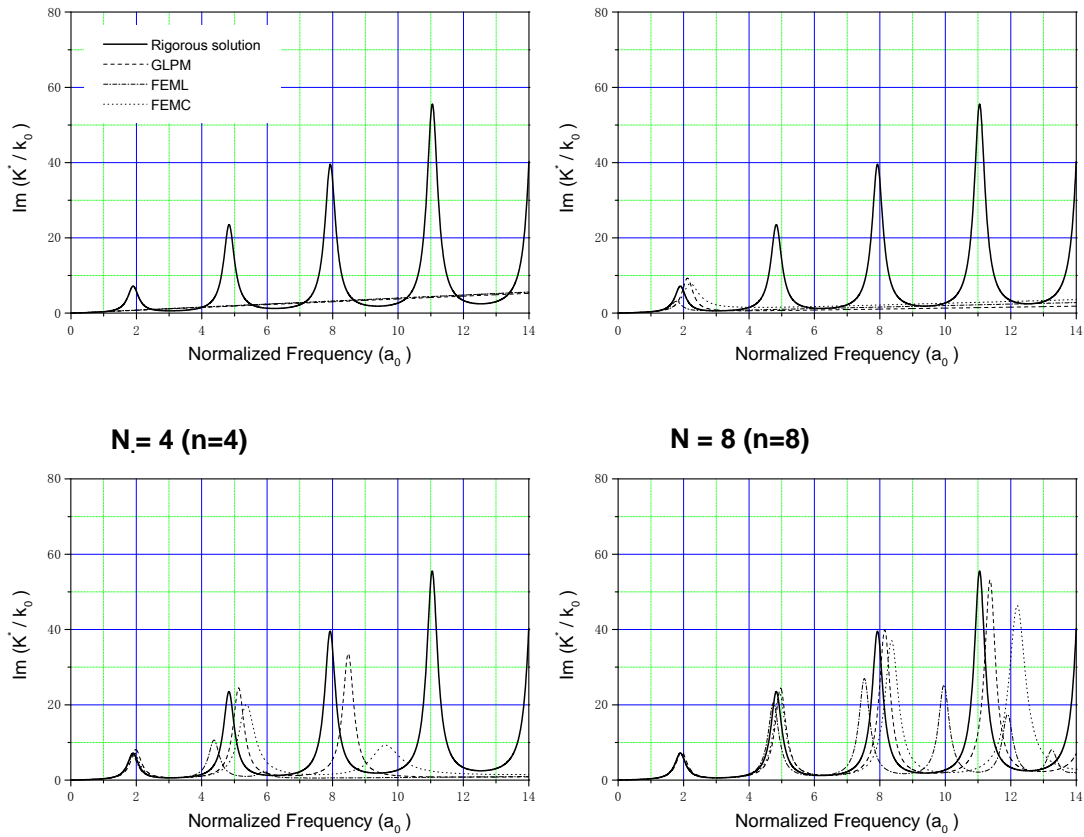


Fig. 6 Normalized impedance functions (imaginary part) at the interface of a rod in the example application of anchors supporting vibrating machinery, using the GLPM with various maximum numbers of units (N). Also shown for comparison are results obtained with the rigorous solution and with conventional finite element models (FEML for lumped mass approach; FEMC for consistent mass approach) with various numbers of DOFs (n).

Masato Saitoh : Lumped parameter models representing impedance functions at the interface of a rod on a viscoelastic medium, *Journal of Sound and Vibration* (in press, available on line), 2010. 11.

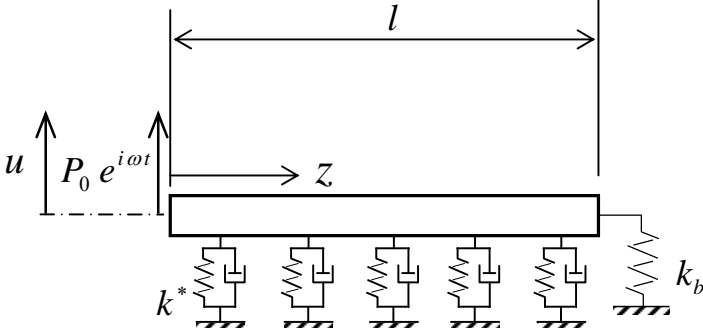


Fig. 7 Shear rod on viscoelastic medium considered in the second example.

Masato Saitoh : Lumped parameter models representing impedance functions at the interface of a rod on a viscoelastic medium, *Journal of Sound and Vibration* (in press, available on line), 2010. 11.

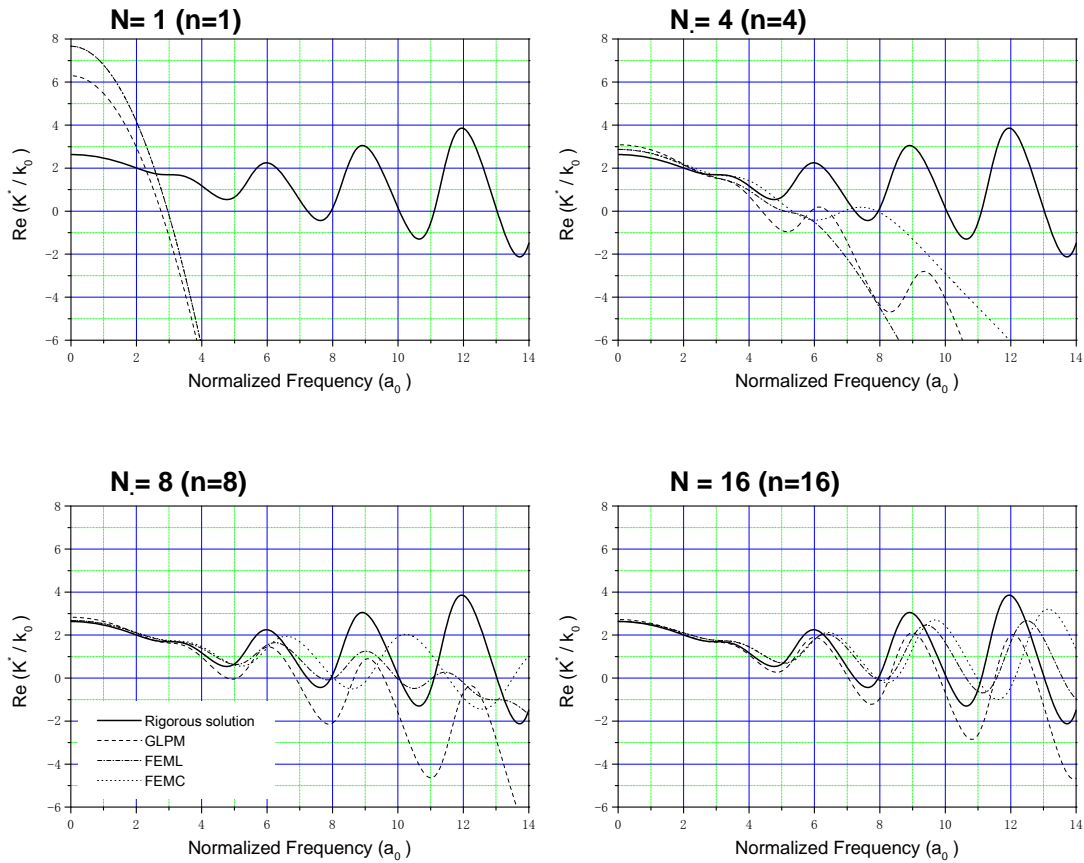


Fig. 8 Normalized impedance functions (real part) at the interface of a rod in the example application of shear keys resisting movement in the transverse direction, using the GLPM with various maximum numbers of units (N). Also shown for comparison are results obtained with the rigorous solution and with conventional finite element models (FEML for lumped mass approach; FEMC for consistent mass approach) with various numbers of DOFs (n).

Masato Saitoh : Lumped parameter models representing impedance functions at the interface of a rod on a viscoelastic medium, *Journal of Sound and Vibration* (in press, available on line), 2010. 11.

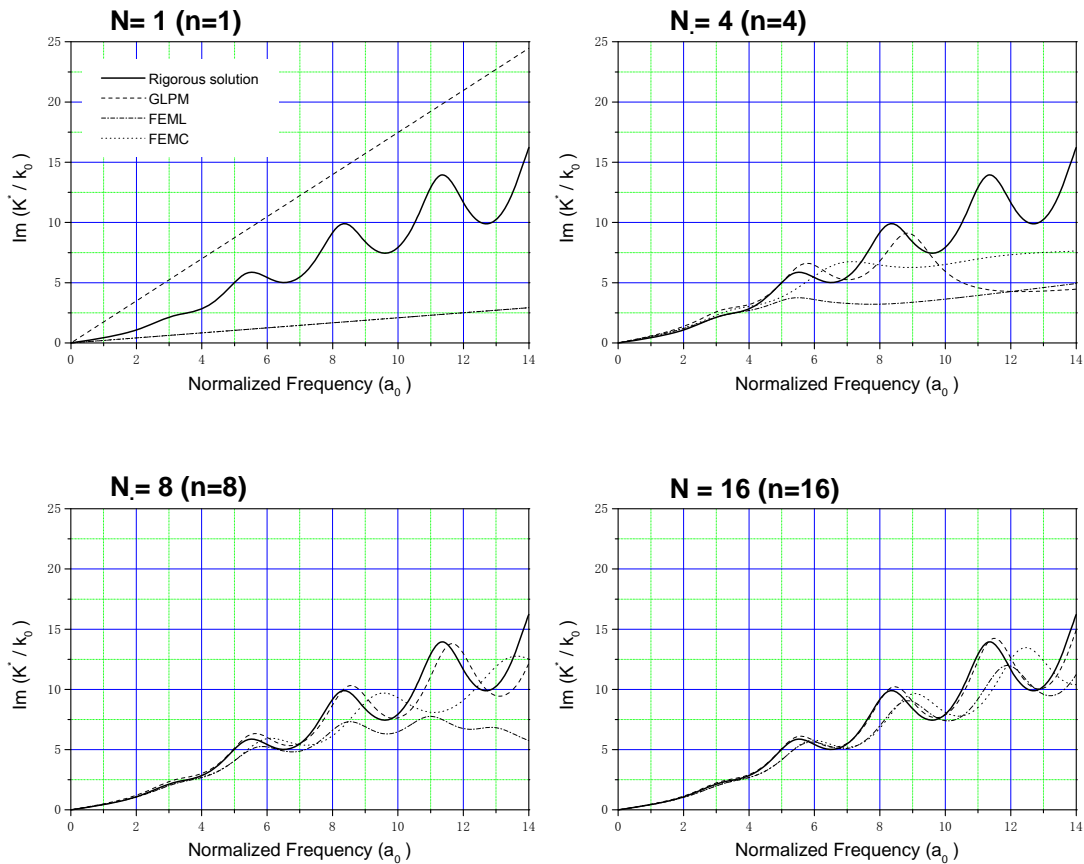


Fig. 9 Normalized impedance functions (imaginary part) at the interface of a rod in the example application of shear keys resisting movement in the transverse direction, using the GLPM with various maximum numbers of units (N). Also shown for comparison are results obtained with the rigorous solution and with conventional finite element models (FEML for lumped mass approach; FEMC for consistent mass approach) with various numbers of DOFs (n).

Masato Saitoh : Lumped parameter models representing impedance functions at the interface of a rod on a viscoelastic medium, *Journal of Sound and Vibration* (in press, available on line), 2010. 11.

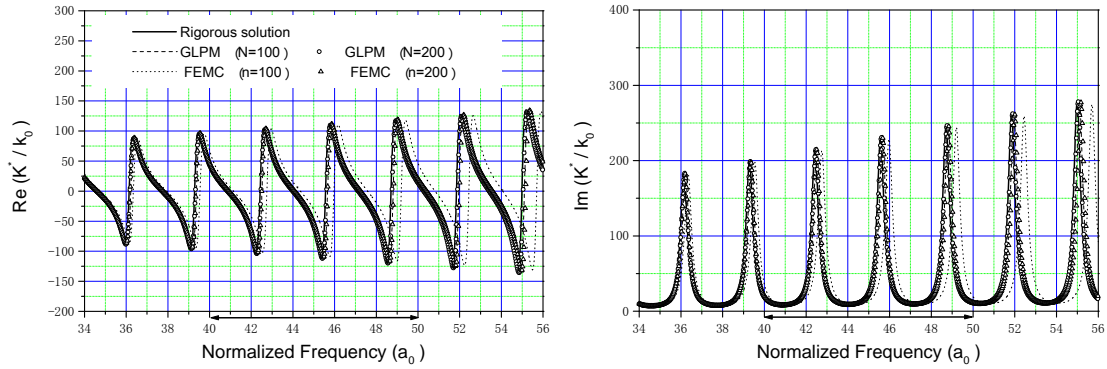


Fig. 10 Normalized impedance functions at the interface of a rod in the previous example application of anchors in a high-frequency region, using the GLPM with various maximum numbers of units ($N=100$ and 200). Also shown for comparison are results obtained with the rigorous solution and the FEMC (FEM for consistent mass approach) with various numbers of DOFs ($n=100$ and 200).

Masato Saitoh : Lumped parameter models representing impedance functions at the interface of a rod on a viscoelastic medium, *Journal of Sound and Vibration* (in press, available on line), 2010. 11.

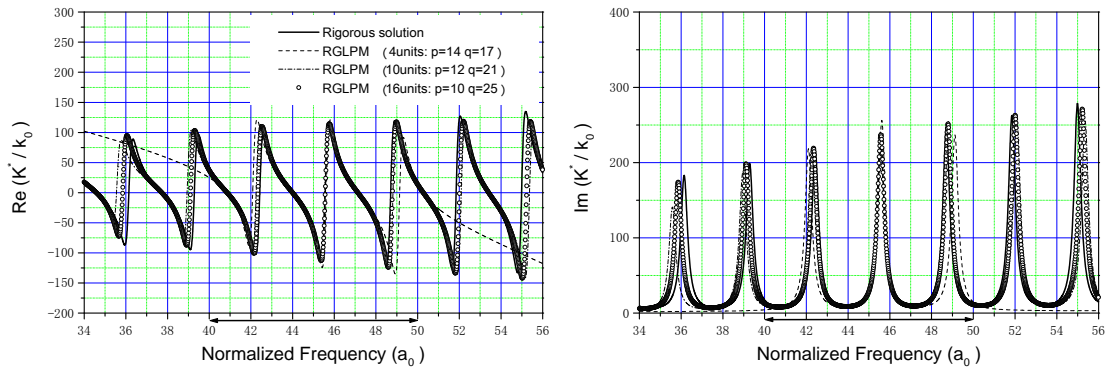


Fig. 11 Partial representation of normalized impedance functions at the interface of a rod in the previous example application of anchors in a particular high-frequency region ($40 \leq a_0 \leq 50$), using the RGLPMs (reduced GLPMs) with various combinations of units associated with selected successive modes ranging from p-th mode to q-th mode.